

Spectra from a magnetic reconnection-heated corona in AGN

B. F. Liu, S. Mineshige, and K. Ohsuga

Yukawa Institute for Theoretical Physics, Kyoto University, Kyoto 606-8502, Japan

bfliu@yukawa.kyoto-u.ac.jp (BFL)

ABSTRACT

We investigate a corona coupled with underlying disk through magnetic field and radiation field, and present emergent spectra. Due to buoyancy the magnetic flux loop emerges from the disk and reconnects with other loops in the corona, thereby releasing the magnetic energy to heat the coronal plasma. The energy is then radiated away through Compton scattering. By studying the energy balance in the corona, transition layer and disk, we determine the fraction (f) of accretion energy dissipated in the corona for given black-hole mass and accretion rate, and then determine the coronal and disk variables. This allows us to calculate emergent spectra through Monte Carlo simulations. The spectra are then determined as functions of black-hole mass and accretion rate. We find two types of solutions corresponding for hard spectrum and soft spectrum. In the hard-spectrum solution, the accretion energy is dominantly dissipated in the corona, supporting a strong corona above a cool disk; The hard X-ray spectral indices are the same for different accretion rate, i.e. $\alpha \sim 1.1$ ($F_\nu \propto \nu^{-\alpha}$). In the soft-spectrum solution, the accretion energy is mainly dissipated in the disk. The coronal temperature and density are quite low. Consequently, the spectra are dominated by the disk radiation peaked in UV and soft X-rays. For low-luminosity systems ($L \lesssim 0.2L_{\text{Edd}}$), there exists only the solution of hard spectra; While for high-luminosity systems ($L \gtrsim 0.8L_{\text{Edd}}$), there exist both solutions of hard and soft spectra. For middle-luminosity systems ($0.2L_{\text{Edd}} \lesssim L \lesssim 0.8L_{\text{Edd}}$), besides the hard spectra, moderately soft spectra composed of an inner soft-spectrum solution and an outer hard-spectrum solution may occur, the softness of which increases with increasing luminosity. The hard spectra are close to the observed spectra in Seyfert galaxies and radio-quiet QSOs. The composite spectra may account for the diversity of broad band spectra observed in narrow-line Seyfert 1 galaxies.

Subject headings: accretion, accretion disks—galaxies: nuclei—X-rays:galaxies

1. Introduction

It is commonly believed that the hard X-ray radiation of active galactic nuclei (AGNs) or galactic black hole candidates (GBHCs) arises from hot gas around accreting black holes, either in forms of hot accretion flow or accretion-disk corona (e.g. Liang & Nolan 1984; Mushotzsky, Done, & Pounds 1993; Narayan, Mahadevan, & Quataert 1998). The structure of hot accretion flows, such as advection-dominated accretion flow (ADAF), has been extensively investigated based on the vertically one-zone approximation (Kato, Fukue, & Mineshige 1998 and references therein). The ADAF model (Ichimaru 1977; Narayan, Yi & Mahadevan 1995; see also Blandford & Begelman 1999; Igumenshchev & Abramowicz 2000 for modifications) can reasonably fit the observed spectra of low luminosity AGNs and X-ray novae in quiescence. Nevertheless, spectral features observed in ordinary AGNs, the big blue bump, the soft X-ray excess and hard X-ray continuum, and the 6.4 keV fluorescent iron lines, show strong observational evidence for hot gas coexisting with cool gas in the vicinity of accreting black hole (e.g., Mushotzky et al. 1993), which is presumably a corona lying above an accretion disk. In disk-corona models, the cold disk is embedded in the hot corona in a plane-parallel slab. Except for the ion-illuminated disk (Deufel & Spruit 2000; Deufel, Dullemond, & Spruit 2002), previous disk corona models for AGNs or GBHCs (Haardt & Maraschi 1991; 1993; Nakamura & Osaki 1993; Svensson & Zdziarski 1994; Dove et al. 1997; Kawaguchi, Shimura, & Mineshige 2001) need to assume a large fraction of accretion energy to be released in the corona though the details of the coronal heating mechanism remain unclear.

Detailed investigation on the interaction between an accretion disk and a friction-heated corona (Liu et al. 2002b) shows that the energy deposit in the corona is not enough to keep itself hot above the disk against strong Compton cooling in AGN systems. Other heating besides the viscous one is required to maintain such a hot corona lying above the disk and to produce the observed X-ray luminosity. Comparison of the thermal energy capacity in the corona and observed power of AGNs also shows energy shortage in the corona (Merloni & Fabian 2001). One promising mechanism to heat the corona may be the magnetic reconnection (e.g. Di Matteo 1998; Di Matteo, Celotti, & Fabian 1999; Miller & Stone 2000; Machida, Hayashi & Matsumoto 2000) as a result of magnetorotational instabilities in the disk and the buoyancy of the magnetic field (Tout & Pringle 1992; Miller & Stone 2000). Despite of the complex radiation and energy interaction between the disk main body and the corona, magnetic fields seem to play essential role in producing time variations and spatial inhomogeneity (e.g. Kawaguchi et al. 2000).

In a recent study (Liu, Mineshige, & Shibata 2002a, hereafter Paper I), we show

that, the magnetic reconnection can indeed heat the corona to a temperature around 10^9K and produce the observed X-ray luminosity. In the present paper, we describe the model in a more consistent way (Sect.2), and then calculate the spectra from the corona and disk by Monte Carlo simulations. The computational results on the coronal properties and emergent spectra are presented in Sect.3. Discussion on spectra is presented in Sect.4 and our conclusions in Sect.5.

2. The model

In our disk-corona model (Paper I), the disk is assumed to be a classical Shakura & Sunyaev (1973) disk. The corona is a plane-parallel corona which is tightly coupled with the underlying disk. In the disk, magnetic fields are continuously generated by dynamo action. Owing to the buoyancy magnetic flux loops emerge into the corona and reconnect with other loops. Thereby, the magnetic energy carried from the disk is released in the corona as thermal energy. If the density of corona is not high enough, heat is conducted by electrons from the corona to the chromosphere, resulting in mass evaporation. Once the density of corona reaches a certain value, Compton scattering becomes dominant in cooling, and eventually an equilibrium is established between the reconnection heating and Compton cooling, a stationary corona is built up. The equations describing these processes in the corona and at the interface of disk and corona are (see Paper I),

$$\frac{B^2}{4\pi}V_A \approx \frac{4kT}{m_e c^2} \tau^* cU_{\text{rad}}, \quad (1)$$

$$\frac{k_0 T^{\frac{7}{2}}}{\ell} \approx \frac{\gamma}{\gamma - 1} nkT \left(\frac{kT}{m_H} \right)^{\frac{1}{2}}. \quad (2)$$

In stead of τ in Paper I, we introduce effective optical depth, τ^* , which includes the isotropic incident photons undergoing up-scattering in a plane-parallel corona,

$$\tau^* \equiv \lambda_\tau \tau = \lambda_\tau n \sigma_T \ell \quad (3)$$

with λ_τ being order of unit.

Eq.(1) and Eq.(2) determine the temperature and density in the corona as function of energy densities of magnetic field and radiation field.

The magnetic field strength B is derived by assuming equipartition of gas energy and magnetic energy in the disk,

$$\beta \equiv \frac{n_{\text{disk}} k T_{\text{disk}}}{\frac{B^2}{8\pi}} \sim 1. \quad (4)$$

For a radiation pressure-dominated disk,

$$B = 1.47 \times 10^3 \alpha_{0.1}^{-\frac{5}{8}} \beta_1^{-\frac{1}{2}} m_8^{-\frac{5}{8}} [\dot{m}_{0.1} \phi (1 - f)]^{-1} r_{10}^{\frac{9}{16}} G; \quad (5)$$

For a gas pressure-dominated disk,

$$B = 7.18 \times 10^4 \alpha_{0.1}^{-\frac{9}{20}} \beta_1^{-\frac{1}{2}} m_8^{-\frac{9}{20}} [\dot{m}_{0.1} \phi (1 - f)]^{\frac{2}{5}} r_{10}^{-\frac{51}{40}} G, \quad (6)$$

where f is the energy fraction dissipated in the corona; $\phi \equiv 1 - \sqrt{\frac{R_*}{R}}$ and R_* is taken to be the last stable orbit $3R_S$; m_8 , $\dot{m}_{0.1}$, r_{10} , $\alpha_{0.1}$, β_1 are the mass of black hole, the accretion rate, the distance, the viscous coefficient, and the equipartition factor in units of $10^8 M_\odot$, $0.1 \dot{M}_{\text{Edd}}$, $10R_S$, 0.1, and 1, respectively.

The energy density of soft photon field, U_{rad} , is contributed from both intrinsic disk radiation $U_{\text{rad}}^{\text{in}}$ and reprocessed radiation $U_{\text{rad}}^{\text{re}}$ of backward Compton emission from the corona

$$\begin{aligned} U_{\text{rad}}^{\text{in}} &= aT_{\text{eff}}^4 = \frac{4}{c} \frac{3GM\dot{M}(1-f)\phi}{8\pi R^3} \\ &= 1.14 \times 10^5 m_8^{-1} \dot{m}_{0.1} \phi (1-f) r_{10}^{-3} \text{ergs cm}^{-3}, \end{aligned} \quad (7)$$

$$U_{\text{rad}}^{\text{re}} = 0.4 \lambda_u U_B. \quad (8)$$

In Eq.(8), a new factor λ_u is added to the evaluation of seed field in Haardt & Maraschi (1991; 1993), which includes two effects on the soft photon energy, i.e. the dependence on the coronal temperature and optical depth, and the ratio of Alfvén speed to the light speed since the magnetic reconnection releases energy at Alfvén speed while this energy is radiated away at light speed.

Now we are allowed to derive two sets of coronal solutions, corresponding to a radiation pressure-dominated disk and a gas pressure-dominated disk, respectively. From Eqs.(1), (2), (5), and (7), we derive a coronal solution above a radiation pressure-dominated disk,

$$T_1 = 1.36 \times 10^9 \alpha_{0.1}^{-\frac{15}{32}} \beta_1^{-\frac{3}{8}} \lambda_\tau^{-\frac{1}{4}} m_8^{-\frac{3}{32}} [\dot{m}_{0.1} \phi (1 - f)]^{-1} r_{10}^{\frac{75}{10}} \ell_{10}^{\frac{1}{8}} K, \quad (9)$$

$$n_1 = 2.01 \times 10^9 \alpha_{0.1}^{-\frac{15}{16}} \beta_1^{-\frac{3}{4}} \lambda_\tau^{-\frac{1}{2}} m_8^{-\frac{19}{16}} [\dot{m}_{0.1} \phi (1 - f)]^{-2} r_{10}^{\frac{75}{32}} \ell_{10}^{-\frac{3}{4}} \text{cm}^{-3}, \quad (10)$$

where the length of the magnetic loop ℓ_{10} is in unit of $10R_S$.

From Eqs.(1), (2), (6), and (8), we get a coronal solution above a gas pressure-dominated disk,

$$T_2 = 4.86 \times 10^9 \alpha_{0.1}^{-\frac{9}{80}} \beta_1^{-\frac{1}{8}} \lambda_\tau^{-\frac{1}{4}} \lambda_u^{-\frac{1}{4}} m_8^{\frac{80}{8}} [\dot{m}_{0.1} \phi (1 - f)]^{\frac{1}{10}} r_{10}^{-\frac{51}{160}} \ell_{10}^{\frac{1}{8}} K, \quad (11)$$

$$n_2 = 2.55 \times 10^{10} \alpha_{0.1}^{-\frac{9}{40}} \beta_1^{-\frac{1}{4}} \lambda_\tau^{-\frac{1}{2}} \lambda_u^{-\frac{1}{2}} m_8^{-\frac{39}{40}} [\dot{m}_{0.1} \phi (1-f)]^{\frac{1}{5}} r_{10}^{-\frac{51}{80}} \ell_{10}^{-\frac{3}{4}} \text{cm}^{-3}. \quad (12)$$

The fraction of gravitational energy dissipated in the corona can be deduced from its definition (Paper I),

$$f \equiv \frac{F_{\text{cor}}}{F_{\text{tot}}} = \left(\frac{B^2}{4\pi} V_A \right) \left(\frac{3GM\dot{M}\phi}{8\pi R^3} \right)^{-1}. \quad (13)$$

Replacing B and n by Eqs.(5) and (10), we obtain an equation concerning f for a radiation pressure-dominated disk,

$$f = 1.45(1-f)^{-2} \alpha_{0.1}^{-\frac{45}{32}} \beta_1^{-\frac{9}{8}} \lambda_\tau^{\frac{1}{4}} m_8^{-\frac{9}{32}} (\dot{m}_{0.1} \phi)^{-3} r_{10}^{\frac{225}{64}} \ell_{10}^{\frac{3}{8}} \equiv c_1 (1-f)^{-2}. \quad (14)$$

Replacing B and n by Eqs.(6) and (12), we get an equation for a gas pressure-dominated disk,

$$f = 4.70 \times 10^4 (1-f)^{\frac{11}{10}} \alpha_{0.1}^{-\frac{99}{80}} \beta_1^{-\frac{11}{8}} \lambda_\tau^{\frac{1}{4}} \lambda_u^{\frac{1}{4}} m_8^{\frac{11}{80}} (\dot{m}_{0.1} \phi)^{\frac{1}{10}} r_{10}^{-\frac{81}{160}} \ell_{10}^{\frac{3}{8}}. \quad (15)$$

Eq.(15) has solutions for any accretion rate; while Eq.(14) has solutions only if $c_1 < 4/27$, which gives,

$$\frac{\dot{M}}{\dot{M}_{\text{Edd}}} > 0.21 \alpha_{0.1}^{-\frac{15}{32}} \beta_1^{-\frac{3}{8}} \lambda_\tau^{\frac{1}{12}} m_8^{-\frac{3}{32}} \phi^{-1} r_{10}^{\frac{75}{64}} \ell_{10}^{\frac{1}{8}}. \quad (16)$$

This is to say, at high accretion rate, the corona can coexist with a radiation pressure-dominated disk or a gas pressure-dominated disk; while at low accretion rate, the corona can coexist only with the gas pressure-dominated disk. The value of critical accretion rate is related to the distances. For $\alpha = 0.3$, $\beta = 1$, $\lambda_\tau = 2.7$ (see next section), and $M = 10^8 M_\odot$, a radiation pressure-dominated disk exists around distance $R \sim 6R_S$ if $\dot{M} \approx 0.3\dot{M}_{\text{Edd}}$; extends to $50R_S$ if $\dot{M} \approx 1.2\dot{M}_{\text{Edd}}$. We will see in the following section that the spectra from a radiation pressure-dominated disk + corona and from a gas pressure-dominated disk + corona are of much difference.

Solving Eq.(14) (or Eq.(15)) for f for a given black hole mass and accretion rate, we determine the coronal quantities from Eqs.(9) and (10) (or Eqs.(11) and (12)). The disk quantities can also be determined. We are now ready to calculate the spectrum.

3. Spectra calculated from Monte Carlo simulations

3.1. The method of Monte Carlo simulations

We use the Monte Carlo simulations to calculate the emergent spectrum. Our model consists of a cold disk, which produces blackbody radiation at each radius with

temperature T_R ,

$$\sigma T_R^4 = \frac{3GM\dot{M}\phi(1-f)}{8\pi R^3} + \frac{c}{4}U_{\text{rad}}^{\text{re}} \approx \max\left(\frac{3GM\dot{M}\phi(1-f)}{8\pi R^3}, \frac{c}{4}U_{\text{rad}}^{\text{re}}\right). \quad (17)$$

The hot corona lying above the disk is approximated as an optically thin slab with definite electron temperature and scattering optical depth for each radius. The blackbody photons emitted from the cold disk go into the corona, some of them pass through without being scattered, some of them are Compton up-scattered. By tracing the photon's motion in the corona, we separately record the photons emerging from upper and lower boundaries of the slab corona: the former are the ones to be observed and the latter impinge the disk and are reprocessed as blackbody emissions. Since the accretion disk is sufficiently dense, the albedo is neglected in our simulations. The spectra from different radii are added up as the total emergent spectrum.

The method of the Monte Carlo simulation is based on Pozdnyakov, Sobol' & Sunyaev (1978). We restrict our consideration to a thermal corona where the electrons have a Maxwellian distribution, and the Compton scattering is the main cooling process. Since the electron-scattering optical depth in the corona is less than one, we introduce the weight w as described by Pozdnyakov et al. (1978) in order to efficiently calculate the effects of multiple scattering. We first set $w_0 = 1$ for a given soft photon, then calculate the escape probability P_0 of passing through the slab. The quantity of $w_0 P_0$ are the transmitted portion and is recorded to calculate the penetrated spectrum or reprocessed photons according to the escape direction of the photon. The remaining weight $w_1 = w_0(1 - P_0)$ is the portion that undergoes at least one scattering. If we write the escape probability after the n -th scattering as P_n , the quantity $w_n P_n$ is the transmitted portion of photons after the n -th scattering, and is recorded as upward or downward transmitted spectrum. The remaining portion $w_n(1 - P_n)$ undergoes the $(n + 1)$ -th scattering. This calculation is continued until the weight w becomes sufficiently small. The whole process is simulated by the Monte Carlo method.

3.2. Iterative computations for consistency

Once the coronal temperature, the optical depth and the seed soft photons are given, the Monte Carlo simulation can be performed and the Compton scattering spectrum and luminosity coming out from both upside and downside of the corona are obtained. The questions arise, does the upward-outcoming luminosity equal to the gravitation energy released by the accretion? does the energy density of downward-outgoing photon plus intrinsic disk radiation equal to the presumed energy density of seed soft photons? If the seed photon energy and the effective optical depth are

correctly chosen in deriving the corona temperature, density and optical depth, the answers should be affirmative. A consistent model should correctly describe the nature of corona, i.e., the temperature, density, optical depth, etc. so that the simulations give consistent results.

In Paper I, we did not introduce λ_τ and λ_u , which implies $\lambda_\tau = 1$ and $\lambda_u = 1$. This is to say, it is assumed that the reprocessed seed field has energy density $U_{\text{rad}}^{\text{re}} = 0.4B^2/8\pi$ and the effective optical depth is the vertical scattering optical depth $\tau = n\sigma_T\ell$. However, unlike in a spheric geometry, in a plane geometry the actual optical depth (we called it the effective optical depth) should be larger than the vertical one, since the incident photons are isotropic and undergo longer path than ℓ if their directions are not normal to the corona plane. Furthermore, λ_τ is expected to be independent on the system parameters (e.g. accretion rate) since it is only a geometric effect. The energy density of seed photon field contributed from the reprocessed photons, $U_{\text{rad}}^{\text{re}} = 0.4B^2/8\pi$, is estimated for specific range of parameters (e.g. Haardt & Maraschi 1993). The precise value depends on the temperature and optical depth. In order to get consistent results, we need to adjust the presumed energy density of soft photons and the effective optical depth of the scattering medium. This is why we introduce the coefficients λ_τ and λ_u in this study. For simplicity, we set λ_u the same value at all distances though the temperature and density of the corona change a little along the distance as shown in Paper I. This is reasonable since the reprocessed photons are not required to get out of the disk at the same distance where they impinge.

For a given mass of black hole and accretion rate, we first perform the computations for the case of gas pressure-dominated disk. As the first step, we start the computation with initial values $\lambda_\tau = 2$ and $\lambda_u = 1$. For one grid point of radius R , we solve Eq.(15) numerically and obtain a solution for f ; then calculate the corresponding temperature T and density in the corona from Eqs.(11) and (12) and hence the scattering optical depth τ , and the radiation temperature T_R of seed photon field by combining Eqs.(8) and (6). With T , τ , and T_R , we perform the Monte Carlo simulation, record the local upwards luminosity and downwards luminosity. Then we change R to the next grid point and repeat the calculation for f , then for T , τ and T_R , and then Monte Carlo simulation. Finally all the local outgoing photons are added up and the integrated upward luminosity L_{up} and downward luminosity L_{down} are obtained. Meanwhile, the integrated soft photon energy $L_{\text{soft}} = \int_{3R_S}^{50R_S} 2\pi R\sigma T_R^4 dR$ and the released gravitational energy $L_G = \int_{3R_S}^{50R_S} 2\pi R(3GM\dot{M}\phi/8\pi R^3)dR$ are also calculated. The second step is to check the consistency, i.e. $L_{\text{down}} \approx L_{\text{soft}}$ and $L_{\text{up}} \approx L_G$? If yes, we find the correct λ_τ and λ_u and hence the consistent solution for the corona, and stop the computation; if no, set new values for the $(n + 1)$ -th λ_τ and λ_u from the n -th results: $\lambda_{u,n+1} = (L_{\text{down},n}/L_{\text{soft},n})\lambda_{u,n}$ and $\lambda_{\tau,n+1} = (L_{\text{up},n}/L_G)\lambda_{\tau,n}$, then repeat the computation from

the first step until the consistent conditions $L_{\text{down}} \approx L_{\text{soft}}$ and $L_{\text{up}} \approx L_{\text{G}}$ are fulfilled.

In the case of radiation pressure-dominated disk, We solve f from Eq.(14) and then the temperature and density from Eqs.(9) and Eqs.(10). The iteration procedure is similar to the case of gas pressure-dominated disk. The difference is in that we only need to check whether $L_{\text{up}} \approx L_{\text{G}}$ is fulfilled or not, since the contribution to the seed photons from the reprocessed photons are not so important as the intrinsic disk radiations. Thus, λ_u is simply set to unity and is not adjusted during the iteration.

3.3. The self-consistent coronal structure

For given parameters, $M = 10^8 M_{\odot}$, $\alpha = 0.3$, $\ell = 10R_{\text{S}}$, $\beta = 1$, we perform computations for a series of accretion rates. As we discussed in Sect.2, computations show that, for low accretion rates ($\dot{M} \lesssim 0.3\dot{M}_{\text{Edd}}$) there is only gas pressure-dominated solution; for high mass accretion rates there are both gas pressure-dominated and radiation pressure-dominated solutions (say, $\dot{M} = 2\dot{M}_{\text{Edd}}$); for middle accretion rates (say, $\dot{M} = 0.5\dot{M}_{\text{Edd}}$), the gas pressure-dominated solution exists at all distances, while the radiation pressure-dominated solution only exists at small distances. As an example for low accretion rate system, Fig.1 shows how much accretion energy is dissipated in the corona and in the disk for $\dot{M} = 0.1\dot{M}_{\text{Edd}}$. It is shown that almost all the accretion energy is dissipated in the corona; less than one thousandth is dissipated in the disk. The corresponding coronal structure is plotted in Fig.3. The temperature is $\sim 10^9\text{K}$ and the density $\sim 10^9\text{cm}^{-3}$, which are a little lower than that in Paper I since here we take into account the effective optical depth and consistent seed photon field. The effect optical depth is around 0.7 and Compton y -parameter 0.6.

As an example for high accretion rate, Fig.2 and Fig.4 show the energy fraction and coronal structure for an accretion rate of $2\dot{M}_{\text{Edd}}$. For a gas pressure-dominated disk, the coronal temperature and density are almost the same as that for low accretion rates. Only the magnetic field and Alfvén speed increase with accretion rates. This feature is the nature of gas-pressure solutions because f depends on \dot{M} very weakly (see Eq.(15)), so are the temperature (see Eq.(11)) and density (see Eq.(12)). In other words, the coronal structures with a gas pressure-dominated disk underneath are quite uniform. Higher accretion rate only results in faster energy transfer and dissipation in the corona. Such features can be understood as follows. A corona coupled with the disk through the magnetic field and radiation field can self-adjust to an equilibrium at a certain temperature. The magnetic field transports almost all the accretion energy to the corona and releases the energy there through reconnection. At the beginning of reconnection, the electrons are suddenly heated to a very high temperature. Even

though there is no many seed photons to be scattered, the Compton cooling power is still quite strong due to the very high temperature. Thus, the seed photon's energy is greatly amplified. Some fraction of the scattered photons get out of the corona from the backside and are reprocessed in the disk as blackbody radiation. Then the seed photon field is strengthened and the electron temperature decreases due to efficient Compton cooling. The equilibrium is finally reached when the heating by the magnetic reconnection balances the Compton cooling. Such an approach to the equilibrium can be clearly seen from our iterative computations: when λ_u is set to be a small value, the temperature derived from the model is high. With this high T we then obtain high backward-scattered photon luminosity (by the Monte Carlo simulation). Taking this high luminosity as the seed soft photon luminosity, the newly derived T becomes low and hence the soft-photon field contributed from the backward Compton radiation is closer to the true value. By repeating this procedure, the backward-scattered luminosity quickly converges to the seed soft luminosity, and a stationary state is reached.

In table 1 we list for a gas pressure-dominated disk the coefficients λ_u , λ_τ , the emergent luminosity L_{up} , the seed soft photon luminosity L_{soft} , and the amplification factor $A \equiv (L_{\text{up}} + L_{\text{down}})/L_{\text{soft}}$, where L_{down} is the downward/backward Compton luminosity. We find that the Compton amplification factors for different accretion rate are almost the same, $A \sim 2.3$. Soft photons are scattered in the corona, gain energy by a factor of $A - 1 \sim 1.3$ and escape from both sides of the corona. The upward-escaped photons carry a little more energy (L_{up}) than the downward-escaped photons ($\approx L_{\text{soft}}$), the latter is reprocessed as seed photons. The coefficient λ_u for the seed photon field increases with increasing accretion rate. Comparing λ_u and Alfvén speed, we find that λ_u/V_A does not change with \dot{M} . This indicates that the reprocessed photon field is actually proportional to the $U_B(V_A/c)$, the factor V_A/c is due to the lag of magnetic heating (at a speed of V_A) to radiation cooling (at a speed of c). We also find $\lambda_\tau \approx 2.7$, independent on \dot{M} . This is to say, the effective optical depth caused by the slab geometry is as 2.7 times large as the vertical optical depth.

In contrast, for a radiation pressure-dominated disk, a large fraction of the accretion energy dissipates in the disk (see Fig.2), the corona is quite weak with temperature being a few $10^8 K$ and density $\sim 10^8 \text{cm}^{-3}$ (see Fig.4). The seed photons are mainly from the intrinsic disk radiation. The disk and corona are not coupled at the same way as that for a gas pressure-dominated disk. In such a strong disk + weak corona system, the Compton scattering in the corona is quite weak, $\lambda_\tau \approx 1$ and $A \approx 1$. We note that, the energy fraction dissipated in the corona decreases with increasing accretion rate, the temperature and density in the corona also decrease with \dot{M} . This implies that the corona above a radiation pressure-dominated disk is weak at luminous systems.

Table 1: Computational results for a corona above a gas pressure-dominated disk at different accretion rates (where $\dot{M}_{\text{Edd}} \equiv L_{\text{Edd}}/0.1c^2$)

$\dot{M}/\dot{M}_{\text{Edd}}$	A	λ_u	λ_r	L_{up}	L_{soft}
0.01	2.35	1.10	2.74	4.43×10^{43}	3.30×10^{43}
0.05	2.34	1.89	2.72	2.21×10^{44}	1.65×10^{44}
0.1	2.34	2.38	2.71	4.43×10^{44}	3.30×10^{44}
0.5	2.33	4.08	2.68	2.22×10^{45}	1.66×10^{45}
1.0	2.34	5.12	2.68	4.45×10^{45}	3.30×10^{45}
2.0	2.35	6.40	2.68	8.84×10^{45}	6.57×10^{45}

3.4. The emergent spectrum

In last section we show that there are two types of solution for the disk and corona structure. When the accretion disk is presumed to be gas pressure-dominated, we get a solution $f \sim 1$, indicating that most of the gravitational energy is transferred to the corona by strong magnetic field and fast reconnection. The disk is quite cool, with midplane temperature of a few 10^4K . The corona is heated up to a temperature $T \sim 10^9\text{K}$ by the magnetic reconnection, and the density becomes 10^9cm^{-3} through efficient mass evaporation at the interface between the disk and the corona. The dissipated energy in the corona is emitted away by Compton scattering. Part of the seed photons are upward scattered as the emergent spectrum, and part of them are scattered backward, which are reprocessed in the disk surface layer and are emitted as blackbody spectra. Here we assume that the irradiation by the backward Compton radiation does not largely influence the internal structure of a radiative disk but only changes the temperature of the surface layer (for details see Tuchman, Mineshige, & Wheeler 1990). Therefore, the magnetic energy determined by the equipartition in the disk midplane is not affected by the irradiation. Such a highly heated corona produces strong hard X-ray emission. The corona and disk are similar to the “two phases” discussed by Haardt and Maraschi (1993). We call this solution as hard state since its spectrum is hard. Fig.5 shows the spectral energy distribution of hard state for different accretion rates corresponding to different luminosities. [Here we need to point out that the energy conversion coefficient η by accretion is not exactly 0.1 in our case. For given accretion rate we integrate the gravitational energy by $L_G = \int_{R^*}^{50R_S} 2\pi R(3GM\dot{M}\phi/8\pi R^3)dR$. The total luminosity from both side of the disk and corona should be $2L_G$. For $R^* = 3R_S$, $\eta = 2L_G/\dot{M}c^2 \sim 0.07$. Thus, even for $\dot{M} = \dot{M}_{\text{Edd}} \equiv L_{\text{Edd}}/0.1c^2$, the luminosity is less than the Eddington luminosity.] From the figure we see that for different \dot{M} the spectral shapes in the hard state are very similar. The hard X-ray spectral index is

around 1.1, which is a little steeper than that observed in Seyfert galaxies.

The “constant” spectral index is caused by the “uniform” corona. As we show in Sect.3.3, the coronal structure at hard state is nearly independent on the accretion rate and the Compton y -parameter ($\equiv (4kT/m_e c^2)\tau$) hardly changes with \dot{M} . Our computational data show that the radial distributions of y -parameter are indeed the same for different \dot{M} ; y reaches the maximum of $y \sim 0.6$ in the inner region and decreases with distances (see Fig.3). Therefore, the hard-state spectra have similar spectral shapes.

On the other hand, if the disk is presumed to be radiation pressure-dominated, there exists no solution for f at low accretion rate. At high accretion rate, the solution for f is far less than 1, indicating that magnetic buoyancy does not transfer much energy from the disk to the corona, and there is only a weak corona above the disk with low temperature and low density compared to those in the hard state. The gravitational energy is dominantly released in the disk as multi-color blackbody radiation. These photons go through the very weak corona, almost all of them penetrate the corona without being scattered. The spectral energy (νL_ν) peaks at around UV to soft X-rays, dropping steeply at high frequency. We call this solution as the soft state. Fig.6 shows typical spectrum of the soft state for $\dot{M} = 2\dot{M}_{\text{Edd}}$ (corresponding to $L = 1.4L_{\text{Edd}}$). The soft-state spectrum is not much different from pure-disk spectrum. For comparison the hard-state spectrum for the same \dot{M} is also shown in the figure. Obviously, the spectral distributions at soft and hard state are very much different. One may question whether the Bremsstrahlung emissions contribute more to the hard X-rays in this state. Our estimation shows that the Bremsstrahlung emission power is about 5 order of magnitude less than Compton radiation because the density in the soft-state corona is so low.

Furthermore, there are composite solutions, in which the disk is composed of an inner radiation pressure-dominated region and an outer gas pressure-dominated region with a weak inner corona and a strong outer corona above. Whether such a discontinuous disk + corona can dynamically exist is to be studied. Nevertheless, the spectra from such a composite corona + disk show moderate UV-X-ray spectral indices. In Fig.7 we plot such a spectrum for $\dot{M} = 0.5\dot{M}_{\text{Edd}}$ (corresponding to $L = 0.35L_{\text{Edd}}$). It is shown that the inner region produces soft spectra dominated by the disk radiation and the outer region produces typical hard-state spectra dominated by the corona radiation. Thus, the composed spectrum is moderate: its hard X-ray spectrum has the same spectral index as that of hard state; while the ratio of UV and X-ray luminosity, or rather, the UV-X-ray spectral index, is larger than that of hard state. With \dot{M} increases, the inner radiation pressure-dominated region extends outwards and the outer gas-pressure dominated region shrinks. The overall spectrum then becomes softer.

As discussed in Sect.3.3, the hard-state solution can exist in both low- and high-luminosity objects; while a soft-state corona extending to $50R_S$ can only appear at high accretion rate, $\dot{M} \gtrsim 1.2\dot{M}_{\text{Edd}}$ (or $L \gtrsim 0.8L_{\text{Edd}}$). Systems accreting at a rate $0.3\dot{M}_{\text{Edd}} \lesssim \dot{M} \lesssim 1.2\dot{M}_{\text{Edd}}$ (or $0.2L_{\text{Edd}} \lesssim L \lesssim 0.8L_{\text{Edd}}$) can be in a state between hard and soft with UV-X-ray indices varying with accretion rates. Therefore, our model predicts that, two spectral states are possible for accretion rate above $1.2\dot{M}_{\text{Edd}}$; below $0.3\dot{M}_{\text{Edd}}$ only hard state. These features of hard and soft states are summarized in Table 2.

Table 2: The features of disk and corona in the hard and soft spectral states

Spectral state	Range of L	f	Pressure in disk	Typical coronal values T(K) n(cm ⁻³) τ^*	α_{px}	α_X
Hard	Always	~ 1	P_{disk}^g	$\sim 10^9$ $\sim 10^9$ 0.6	~ 1.4	~ 1.1
Soft	$\gtrsim 0.8L_{\text{Edd}}$	< 0.1	P_{disk}^r	Low, decrease with L	> 2	
Moderate	$0.2\text{-}0.8L_{\text{Edd}}$	outer region	hard, inner region	soft	> 1.4	~ 1.1

The parameters in our model are the mass of black hole M , the accretion rate \dot{M} , the thickness of corona ℓ (equivalent of averaged length of magnetic loops), and the equipartition coefficient β . Above study shows the corona structure and spectra in dependence on \dot{M} for given parameters $M = 10^8M_\odot$ and $\ell = 10R_S$ in the region from $3R_S$ to $50R_S$. From the equation concerning f and the solutions of T and $\tau(\propto n\ell)$, we know f , T and τ and hence the spectra only very weakly depend on ℓ , especially at the hard state. In Fig.8 we plot the hard-state spectra for $\ell = 10R_S$ and $\ell = 20R_S$. The two curves overlap. Similarly, the spectra have weak dependence on the mass of black hole. But, considering large change of black-hole mass over a few orders of magnitude, the spectra may be somewhat different. In Fig.8 an example of hard state for $M = 10^5M_\odot$ is shown. Compared to the case for $M = 10^8M_\odot$, the disk component shifts towards high frequency, whereas no obvious difference in the shape of hard X-ray spectra contributed by the corona. For a $10M_\odot$ black hole we expect similar hard X-ray spectra except for the low-frequency component which peaks at soft X-rays due to high effective temperature in the disk. The dependence on β seems large because it directly determines how much of the accretion energy transferred to the corona through magnetic field. Owing to poor knowledge on the equipartition coefficient, we don't discuss this issue here.

4. Discussion on the spectra

The observed spectrum in X-ray 2-20 keV is close to a power law, with an averaged spectral index $\approx 0.7 \pm 0.15$ for Seyfert galaxies (Mushotzky 1984; Turner & Pounds 1989). Taking into account the deconvolution of the Compton reflection hump around $\approx 30\text{keV}$ (George & Fabian 1991; Williams et al. 1992; Mushotzki et al. 1993; Petrocci et al. 2000), the spectral index of the underlying power law for Seyfert galaxies is 0.9 to 1.0 (e.g. Nandra & Pounds 1994; Pounds et al. 1990). The X-ray spectral index for radio-quiet QSOs is slightly higher, $\alpha_X \approx 1.0$ (e.g. George et al. 2000). The observed broad band spectral index measured between 2500\AA and 2keV is 1.25 for Seyferts (Walter & Fink 1993) and 1.5 for QSOs (Yuan et al. 1998). Our model shows that at hard state the X-ray spectral indices between 2-20keV are around 1.1. The spectral indices between the hump (around UV) and 2keV , α_{px} , are around 1.4. The hard-state spectra are roughly in agreement with the observed spectra of Seyfert galaxies and QSOs.

The composite spectrum, which occurs only at relative high accretion rates and becomes more and more close to the soft spectrum with increase of \dot{M} , may explain the diversity of spectra observed in narrow-line Seyfert 1 galaxies (NLS1s). NLS1 is a subgroup of Seyfert 1 galaxies, but is characterized by large soft X-ray excess (see Fig.1 in Boller 2000). It has been proposed that black hole masses are systematically smaller, while luminosities are comparable to those of other Seyfert 1s, leading to large L/L_{Edd} in NLS1s (Osterbrock & Pogge 1985; Boller, Brandt, & Fink 1996; Mineshige et al. 2000). Our composite soft spectra may correspond for various spectra observed in NLS1s. Furthermore, a small fraction of QSOs with optical-X-ray spectral index $\alpha_{\text{oX}} \gtrsim 2$ are observed (Yuan et al. 1998), which may be interpreted by our composite soft spectra. Comparison with GBHCs are another interesting, outstanding issue but is beyond the present investigation.

Compared with the excellent work of Haardt & Maraschi (1993, hereafter HM93), our hard-state results are quite similar to theirs. This is easy to understand, since our study on the interaction between the disk and corona shows $f \sim 1$, which is a basic assumption in HM93. We also find soft-state spectra, where the corona is not coupled with the disk in the same way as that in HM93. Therefore, the spectra are different from HM93. Despite of the complexity, the basic differences can be briefly described as follows. HM93 consider the coupling between the disk and the corona through seed photons, which gives a relation between the soft radiation temperature T_R , the corona temperature T , and the optical depth τ , i.e. $F_1(T_R, T, \tau) = C_1$. They find for $5eV < T_R < 50eV$ and $0.01 < \tau < 1$, the relation can be approximated as $(16\Theta^2 + 4\Theta)\tau = 0.6$ (where $\Theta \equiv kT/m_e c^2$). For given T_R and τ , T is determined by this

approximation, and then the spectrum is obtained from the Monte Carlo simulations. By changing T_R and τ within the limited range, they got somewhat similar spectral indices. In our model, we also consider the energy coupling between the disk and corona through the soft photons, i.e. $F_1(T_R, T, \tau) = C_1$. In addition, we consider the coupling by the magnetic field and get the second relation, $F_2(T_R, T, \tau) = C_2(M, \dot{M}, f)$. Supplemented by the mass evaporation, we have the third relation, $F_3(T, \tau) = C_3$. Therefore, we uniquely determine T_R, T , and τ for given f , M , and \dot{M} . Then, we perform the Monte Carlo simulation and obtain the spectrum and upward luminosity $L(M, \dot{M}, f)$. Using the fourth relation of that the luminosity equals to the accretion energy, i.e., $L(M, \dot{M}, f) = L_G(M, \dot{M})$, we can also determine f . HM93 also take into account other factors like anisotropy of the seed photons. Here we concentrate on the underlying physics in order to determine the corona variables.

5. Conclusion

We improved our simple model presented in Paper I by introducing adjustable coefficients for the energy density of the coupled seed photons and for the optical depth of plane-parallel corona. For given mass of black hole, accretion rate, and presumed coefficients, the model can determine the energy fraction dissipated in the corona and hence determine the structure of both the corona and disk. Then, we perform Monte Carlo simulations to trace the motion of photons in the corona and record the upward photons (emergent luminosity) and the backward photons. By comparing the presumed seed photon energy and the sum of intrinsic disk radiation and backward radiation energy, we adjust the coefficient of soft photon field and; by comparing the total accretion energy and the simulating emergent luminosity, we modify the effective optical depth in the slab geometry. Repeating this procedure, we finally obtain the self-consistent solutions for the corona and also for the disk, both of which are coupled by the magnetic field and the radiation field.

We find two types of solutions for the disk and corona structure, corresponding for the hard-state and soft-state spectra. In the hard-state solution, the accretion disk is gas pressure-dominated. Most of the accretion energy is transferred to the corona by the magnetic field, and the intrinsic disk radiation is very weak. The corona and disk are tightly coupled through the radiation field and, consequently, the hard X-ray spectral indices are almost fixed at $\alpha \sim 1.1$. In the soft-state solution, most of the accretion energy is dissipated in the disk and thus the disk is radiation pressure-dominated. The corona is weak, characterized by lower temperature and density, and is no longer strongly coupled with the disk through seed photons. The emergent spectral energy comes mainly from the un-scattered intrinsic disk radiation, peaking at UV and

soft X-rays. The soft states appear at only very high luminosity; while hard states appear at both high and low luminosities. A state between soft and hard, composed of an inner soft-state solution and an outer hard-state solution, is also possible for a moderately luminous system. Our model predicts that the spectra is hard from low-luminosity objects with $L \lesssim 0.2L_{\text{Edd}}$; While the spectra can be either hard or soft from high-luminosity objects with $L \gtrsim 0.8L_{\text{Edd}}$. Spectra from objects with luminosity $0.2L_{\text{Edd}} \lesssim L \lesssim 0.8L_{\text{Edd}}$ can be hard, and can also be moderately soft, which is softer at higher luminosity.

We would like to thank R. Matsumoto for providing part of the simulation code. We are grateful to the anonymous referee for his/her detailed and helpful comments. BFL thanks for support by Japan Society for the Promotion of Science. This work is partially supported by the Grants-in Aid of the Ministry of Education, Culture, Sports, Science and Technology of Japan (P.01020 to B.F.L; 13640238 and 14079205 to S.M.).

REFERENCES

- Blandford, R.D., & Begelman, M.C. 1999, MNRAS, 303, L1
- Boller, Th., 2000, NewA Rev., 44, 387
- Boller, Th., Brandt, W. N., & Fink, H, 1996, A&A, 305, 53
- Deufel, B., & Spruit, H. C., 2000, A&A, 362,1
- Deufel, B., Dullemond, C. P., & Spruit, H. C., 2002, A&A, 387, 907
- Di Matteo, T., 1998, MNRAS, 299, L15
- Di Matteo, T., Celotti, A., & Fabian, A. C., 1999, MNRAS, 304, 809
- Dove, J. B., Wilms, J., Maisack, M., & Begelman, M. C., 1997, ApJ, 487, 759
- George, I. M., & Fabian, A. C., 1991, MNRAS, 249, 352
- George, I. M. et al., 2000, ApJ, 531, 52
- Haardt, F., & Maraschi, L., 1991, ApJ, 380, L51
- Haardt, F., & Maraschi, L., 1993, ApJ, 413, 507
- Ichimaru, S. 1977, ApJ, 214, 840

- Igumenshchev, V. & Abramowicz, M.A. 2000, *ApJS*, 130, 463
- Kato, S., Fukue, J. & Mineshige, S. 1999, *Black-Hole Accretion Disks* (Kyoto: Kyoto Univ. Press).
- Kawaguchi, T., Mineshige, S., Machida, M., Matsumoto, R. & Shibata, K., 2000, *PASJ*, 52, L1
- Kawaguchi, T., Shimura, T., & Mineshige, S. 2001, *ApJ*, 546, 966
- Liang, E. P., & Nolan, P. L., 1984, *Space Sci. Rev.*, 38, 353
- Liu, B. F., Mineshige, S., & Shibata, K., 2002a, *ApJ*, 572, L173 (Paper I)
- Liu, B. F., Mineshige, S., Meyer, F., Meyer-Hofmeister, E., & Kawaguchi, T., 2002b, *ApJ*, 575, 117
- Liu, F. K., Meyer, F., & Meyer-Hofmeister, E., 1995, *A&A*, 300, 823.
- Machida, M., Hayashi, M. R., & Matsumoto, R., 2000, *ApJ*, 532, L67
- Merloni, A., & Fabian, A. C., 2001, *MNRAS*, 321, 549
- Miller, K. A., & Stone, J. M., 2000, *ApJ*, 534, 398
- Mineshige, S., Kawaguchi, T., Takeuchi, M., & Hayashida, K, 2000, *PASJ*, 52, 499
- Mushotzsky, R. F., 1984, *Adv. Space. Res*, 3,157
- Mushotzsky, R. F., Done, C., & Pounds, K. A., 1993, *ARA&A*, 31, 717
- Nakamura, K., & Osaki, Y., 1993, *PASJ*, 45, 775
- Nandra, K., & Pounds, K. A., 1994, *MNRAS*, 268, 405
- Narayan, R., Yi, I., & Mahadevan, R., 1995, *Nature*, 374, 623
- Narayan, R., Mahadevan, R., & Quataert, E., 1998, in *The Theory of Black Hole Accretion Disks*, ed. M. A. Abramowicz, G. Bjornsson, & J. E. Pringle (Cambridge: Cambridge Univ. Press), 148
- Osterbrock, D. E. & Pogge, R. W., 1985, *ApJ*, 297, 166
- Pozdnyakov, L. A., Sobol', I. M., & Sunyaev, R. A., 1978, *Soviet Astron.*, 21, 708
- Petrucci, P. O. et al., 2000, *ApJ*, 540, 131

- Pounds, K. A., Nandra, K., Steward, G. C., George, I. M., & Fabian, A. C., 1990, *Nature*, 344, 132
- Shakura, N. I., & R. A. Sunyaev, 1973, *A&A*, 24, 337
- Shibata, K., Tajima, T., Steinolfson, R. S., & Matsumoto, R., 1989, *ApJ*, 345, 584
- Shibata, K., & Yokoyama, T. 1999, *ApJ*, 526, L49
- Shmeleva, O. P., & Syrovatskii, S. I., 1973, *Solar Physics*, 33, 341
- Spitzer, L., 1962, *Physics of Fully Ionized Gases* (2nd ed.; New York: Interscience)
- Svensson, R., & Zdziarski, A. A., 1994, *ApJ*, 436, 599
- Tout, C. A., & Pringle, J. E., 1992, *MNRAS*, 259, 604
- Tuchman, Y., Mineshige, S., & Wheeler, J. C., 1990, *ApJ*, 359, 164
- Turner, T. J., & Pounds, K. A., 1989, *MNRAS*, 240, 833
- Walter, R. & Fink, H. H., 1993, *A&A*, 274, 105
- Williams, O. R., et al., 1992, *ApJ*, 389, 157
- Yokoyama, T., & Shibata, K., 2001, *ApJ*, 549, 1160
- Yuan, W., Brinkmann, W., Siebert, J., & Voges, W., 1998, *A&A*, 330, 108

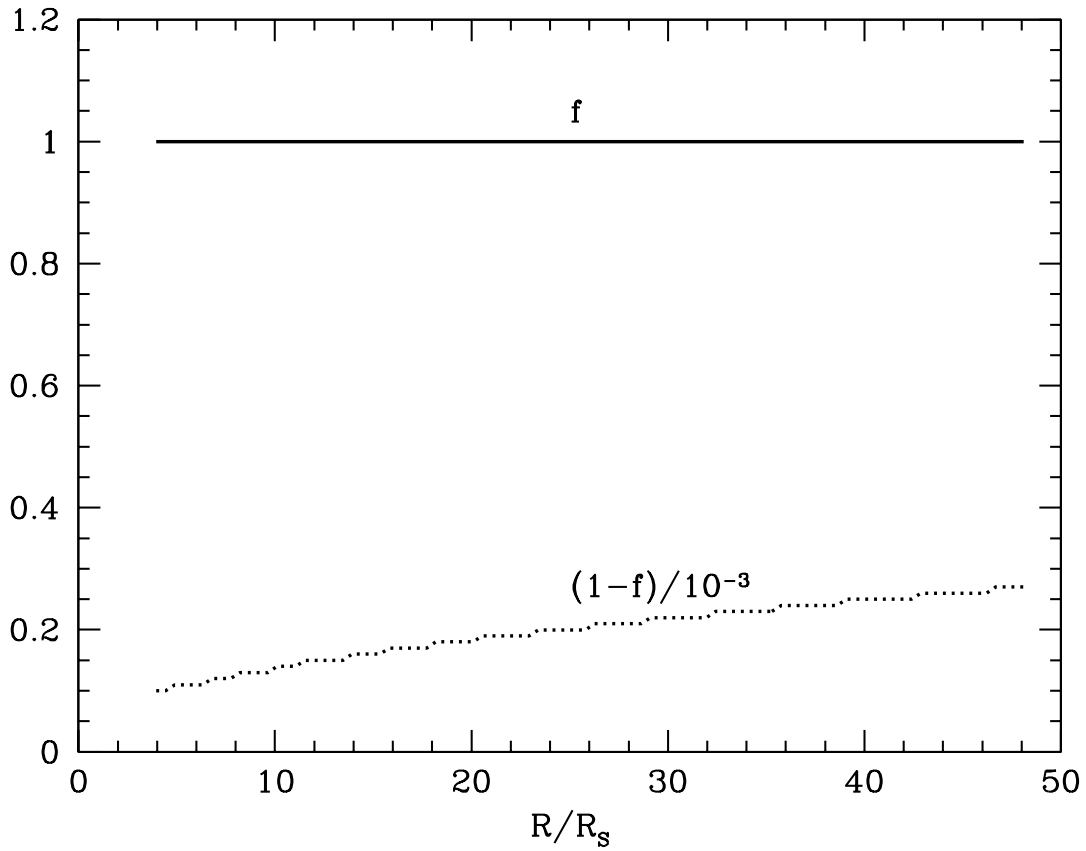


Fig. 1.— Accretion-energy fractions dissipated in the corona, f , and in the disk, $1 - f$, for $M = 10^8 M_\odot$ and $\dot{M} = 0.1 \dot{M}_{\text{Edd}}$ (corresponding to $L = 0.07 L_{\text{Edd}}$). The disk is gas pressure-dominated. The figure shows that most of the accretion energy is dissipated in the corona. Only a very small fraction is dissipated in the disk.

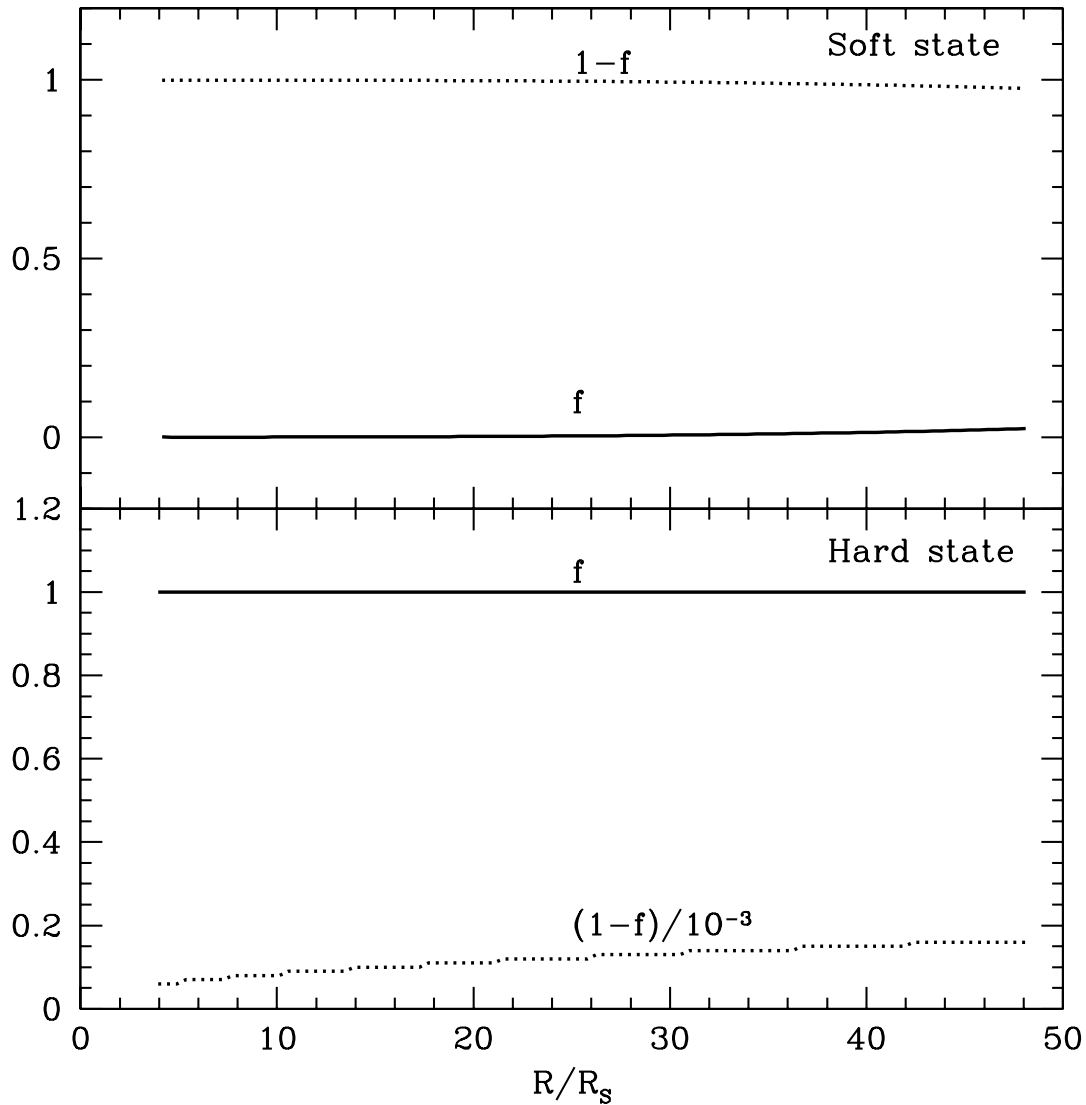


Fig. 2.— Two solutions of f for $M = 10^8 M_\odot$ and $\dot{M} = 2.0\dot{M}_{\text{Edd}}$ (corresponding to $L = 1.4L_{\text{Edd}}$). The lower panel shows that for a gas pressure-dominated disk (hard state) a large fraction of accretion energy is dissipated in the corona; The upper panel shows that for a radiation pressure-dominated disk (soft state) only a very small fraction of accretion energy is transported to the corona, while most of the energy is dissipated in the disk.

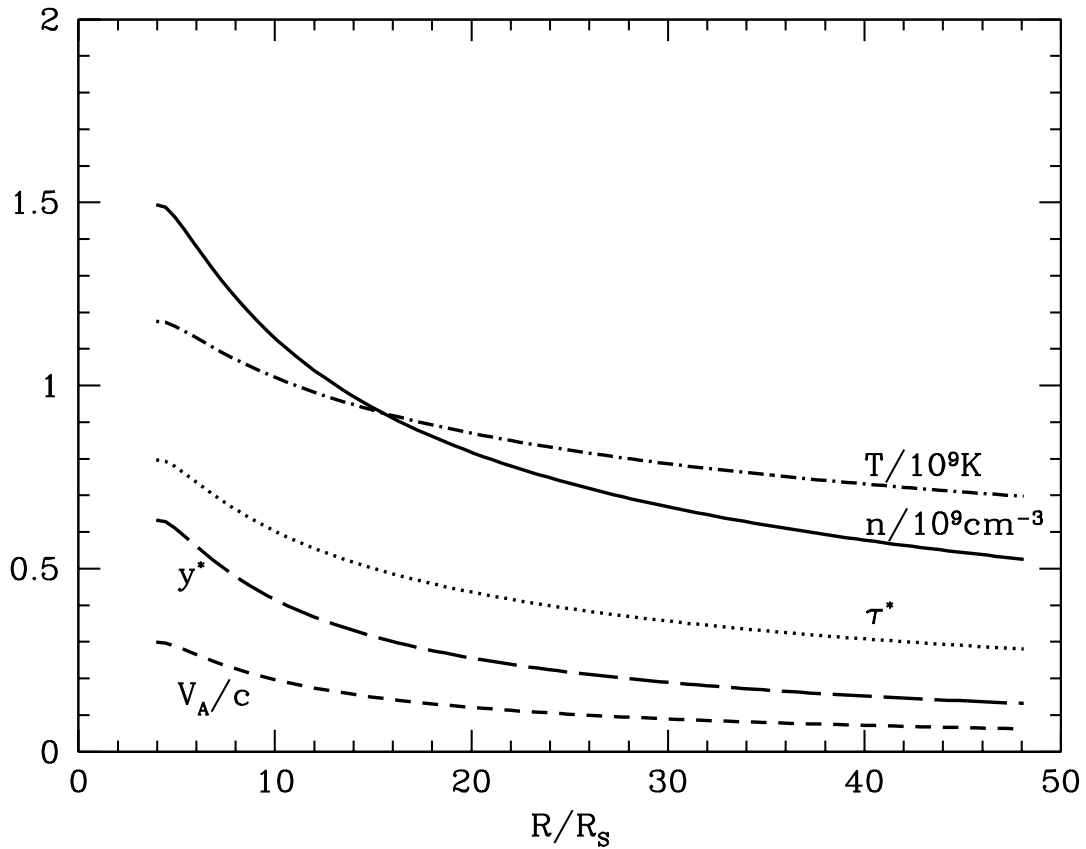


Fig. 3.— Coronal quantities along distance for $M = 10^8 M_\odot$ and $\dot{M} = 0.1 \dot{M}_{\text{Edd}}$ (corresponding to $L = 0.07 L_{\text{Edd}}$). The corona is above a gas pressure-dominated disk with energy fraction channeled to the corona $f \sim 1$ shown in Figure 1. The coronal temperature is around 10^9K and density around 10^9cm^{-3} . The effective optical depth τ^* and Compton y -parameter y^* are also shown, which hardly change with the luminosity.

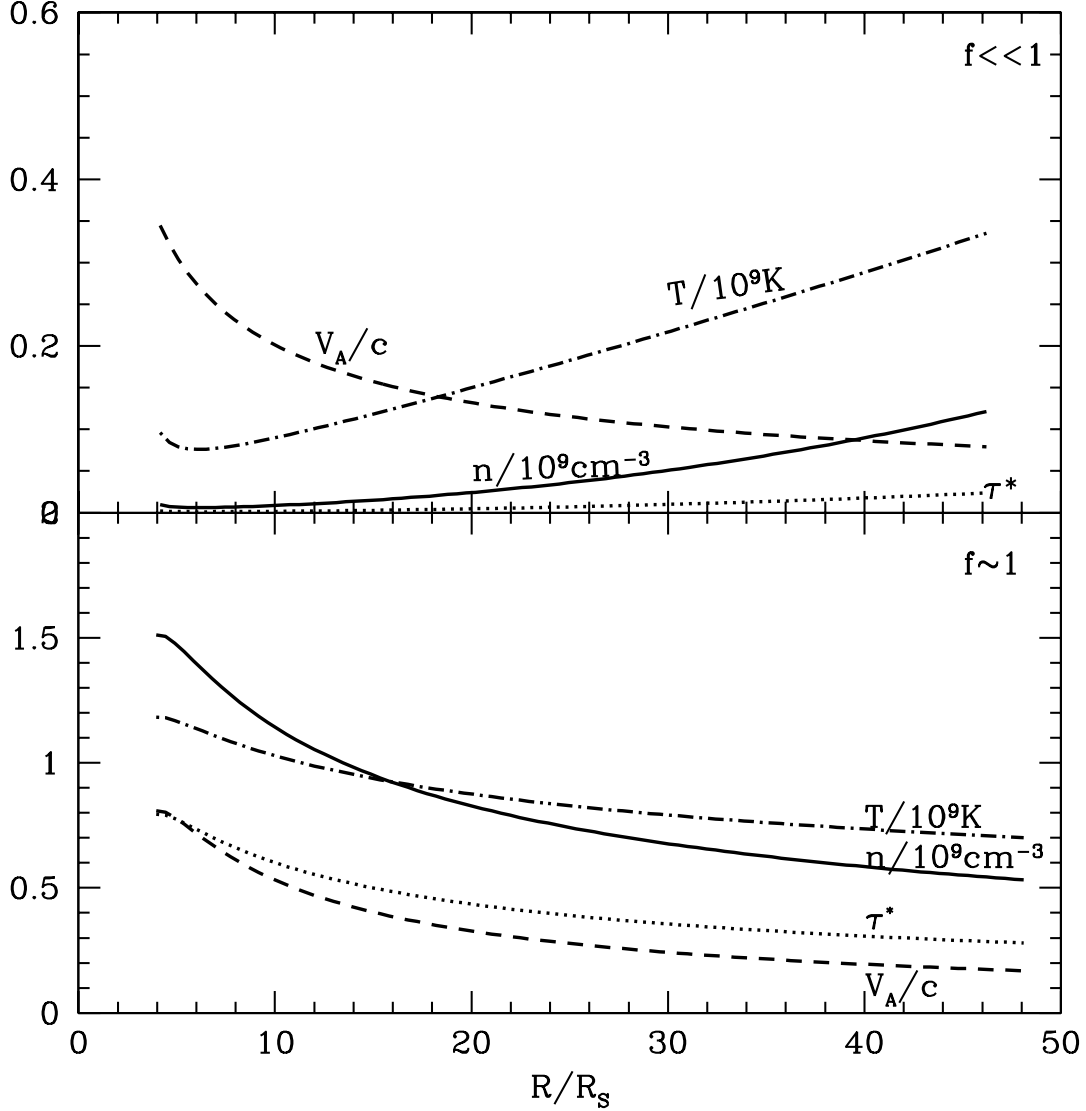


Fig. 4.— Coronal quantities along distance for $M = 10^8 M_\odot$ and $\dot{M} = 2.0 \dot{M}_{\text{Edd}}$ (corresponding to $L = 1.4 L_{\text{Edd}}$). The lower panel shows structure of the corona above a gas pressure-dominated disk with energy fraction channeled to the corona $f \sim 1$. The temperature and density are almost the same as that for small \dot{M} shown in Figure 3; while the Alfvén speed is larger at higher \dot{M} . The upper panel shows structure of the corona above a radiation pressure-dominated disk. Since most of the accretion energy is dissipated in the disk, the corona is weak with temperature \sim a few $10^8 K$ and density $\lesssim 10^8 \text{cm}^{-3}$ in the inner region. In the outer region, T and n are relatively high due to a little larger fraction of local accretion energy is transferred to the corona.

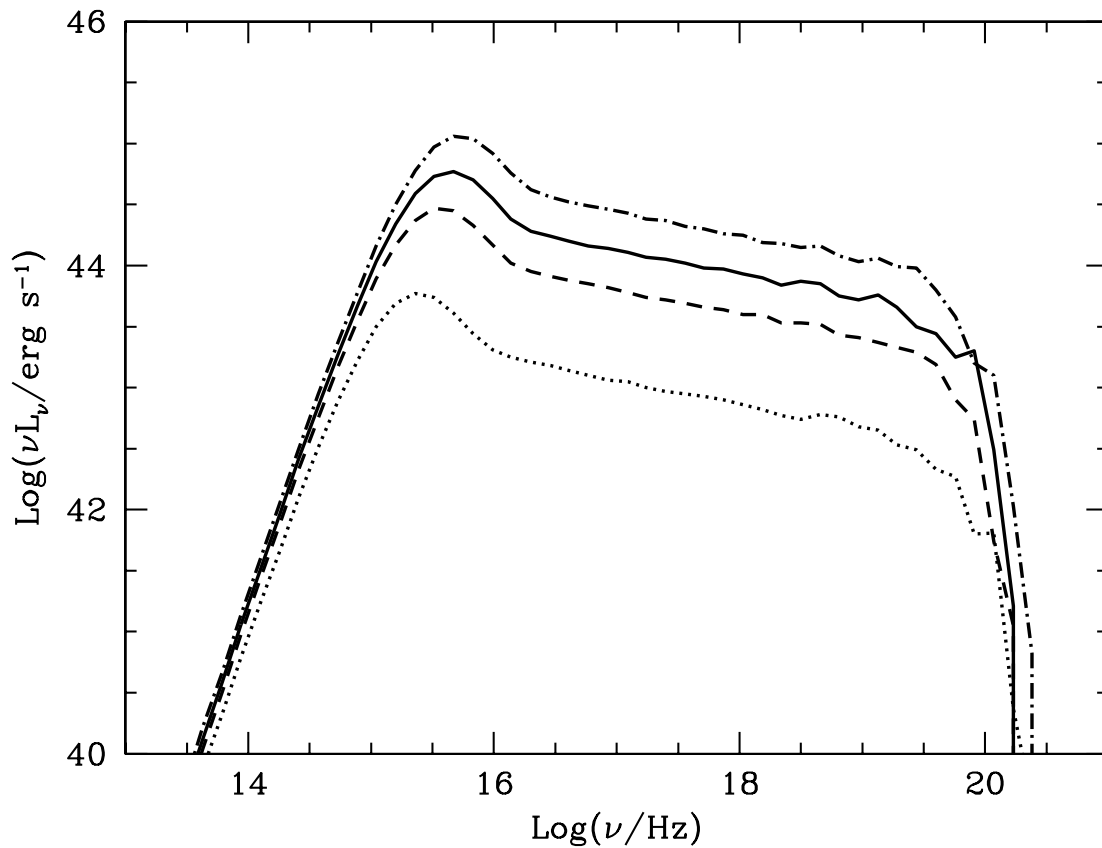


Fig. 5.— The hard-state spectra from a disk and corona around a black hole of $10^8 M_\odot$ at accretion rates $\dot{M} = 0.1\dot{M}_{\text{Edd}}$ (or $L = 0.07L_{\text{Edd}}$; Dotted curve); $\dot{M} = 0.5\dot{M}_{\text{Edd}}$ (or $L = 0.35L_{\text{Edd}}$; Dashed curve); $\dot{M} = 1.0\dot{M}_{\text{Edd}}$ (or $L = 0.7L_{\text{Edd}}$; Solid curve); and $\dot{M} = 2.0\dot{M}_{\text{Edd}}$ (or $L = 1.4L_{\text{Edd}}$; Dash-dotted curve). The hard X-ray emission is quite strong with a spectral index around 1.1. The spectral energy distributions are similar for different luminosities.

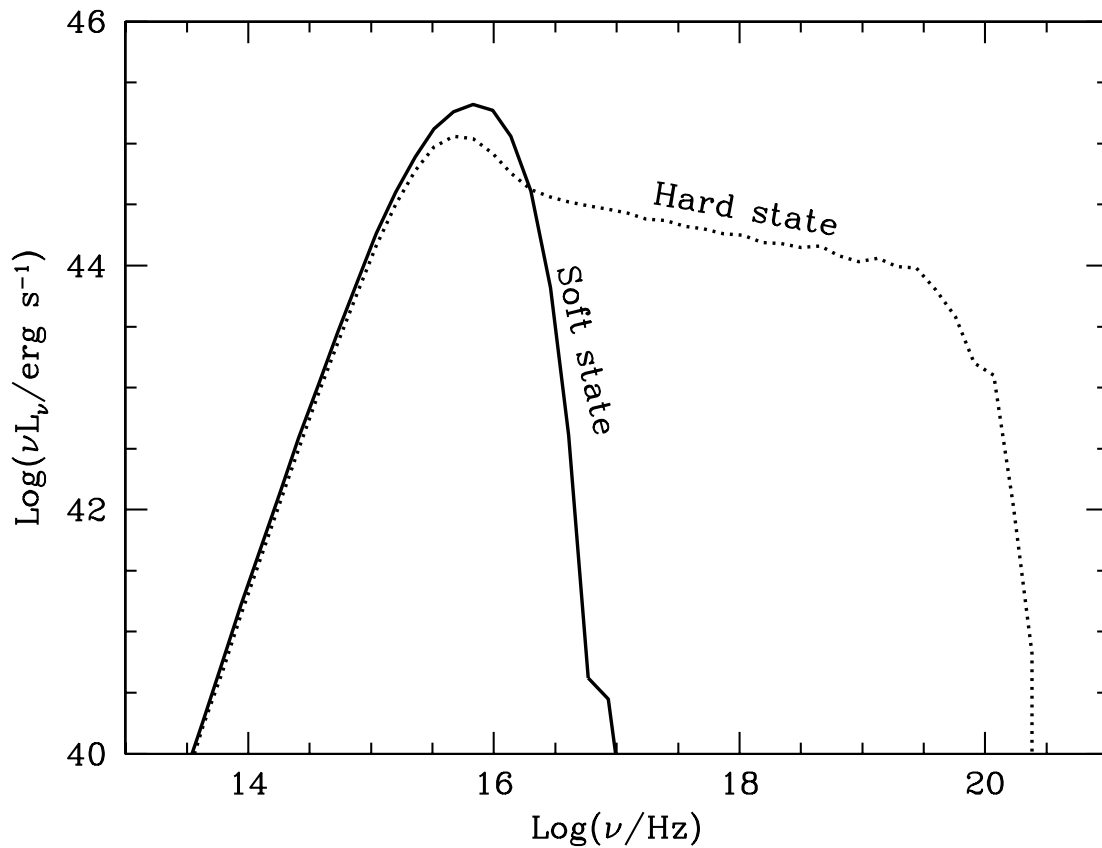


Fig. 6.— The soft-state spectrum (Solid curve) from a disk and corona around a black hole of $10^8 M_\odot$ at accretion rate $\dot{M} = 2.0\dot{M}_{\text{Edd}}$ (or $L = 1.4L_{\text{Edd}}$). The spectral energy distributes dominantly in UV and soft X-ray since most of the accretion energy is dissipated in the disk. For comparison the corresponding hard-state spectrum is also shown in the figure (Dotted curve). Obviously, the X-ray spectra at soft state and hard state are of much difference.

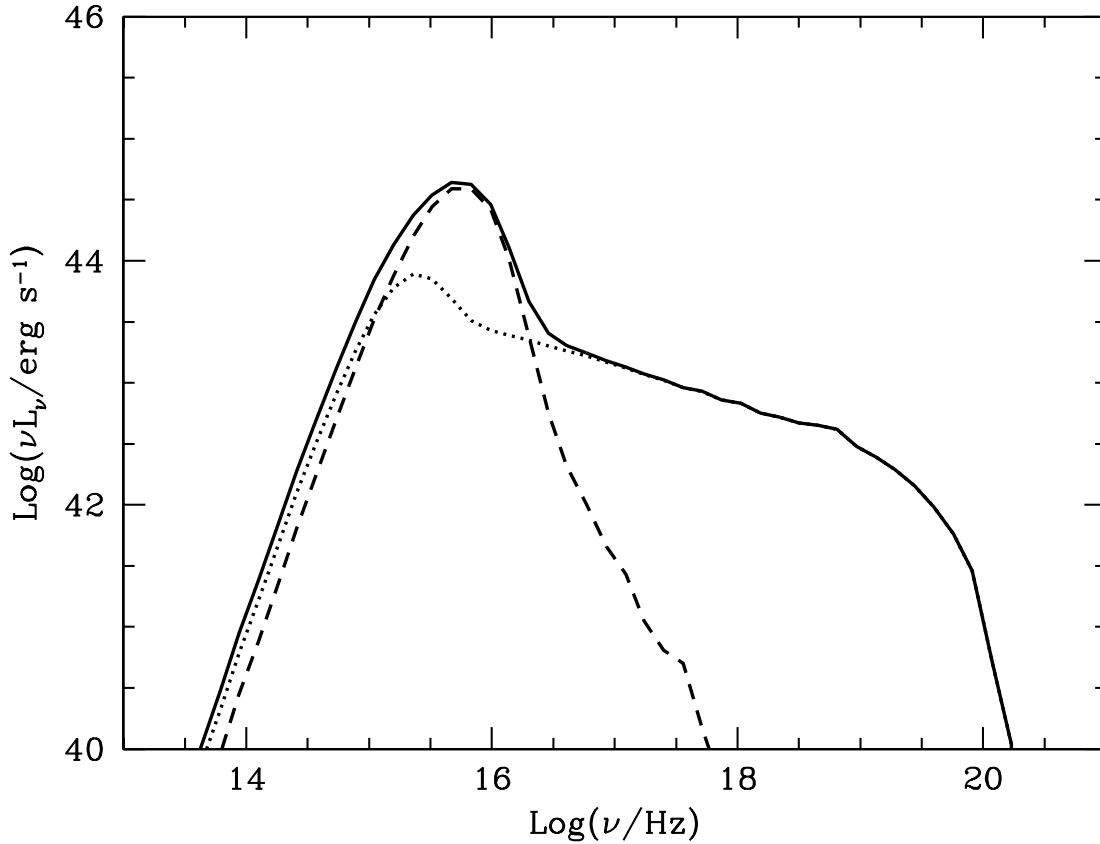


Fig. 7.— The composed spectrum from a disk and corona around a black hole of $10^8 M_\odot$ at accretion rate $\dot{M} = 0.5\dot{M}_{\text{Edd}}$ (or $L = 0.35L_{\text{Edd}}$). The disk is radiation pressure-dominated in the inner region until $19R_S$ and gas pressure-dominated in the outer region, and hence the overlying corona is weak in the inner region and strong in the outer region. Dashed curve shows spectral energy distribution from the inner region, which is obviously contributed by the disk radiation; Dotted curve shows the contribution by the outer region, which is a typical radiation-coupled hard-state spectrum; The solid curve shows the total spectrum. The overall spectral energy distribution is between the hard state and soft state, and the softness increases with accretion rate.

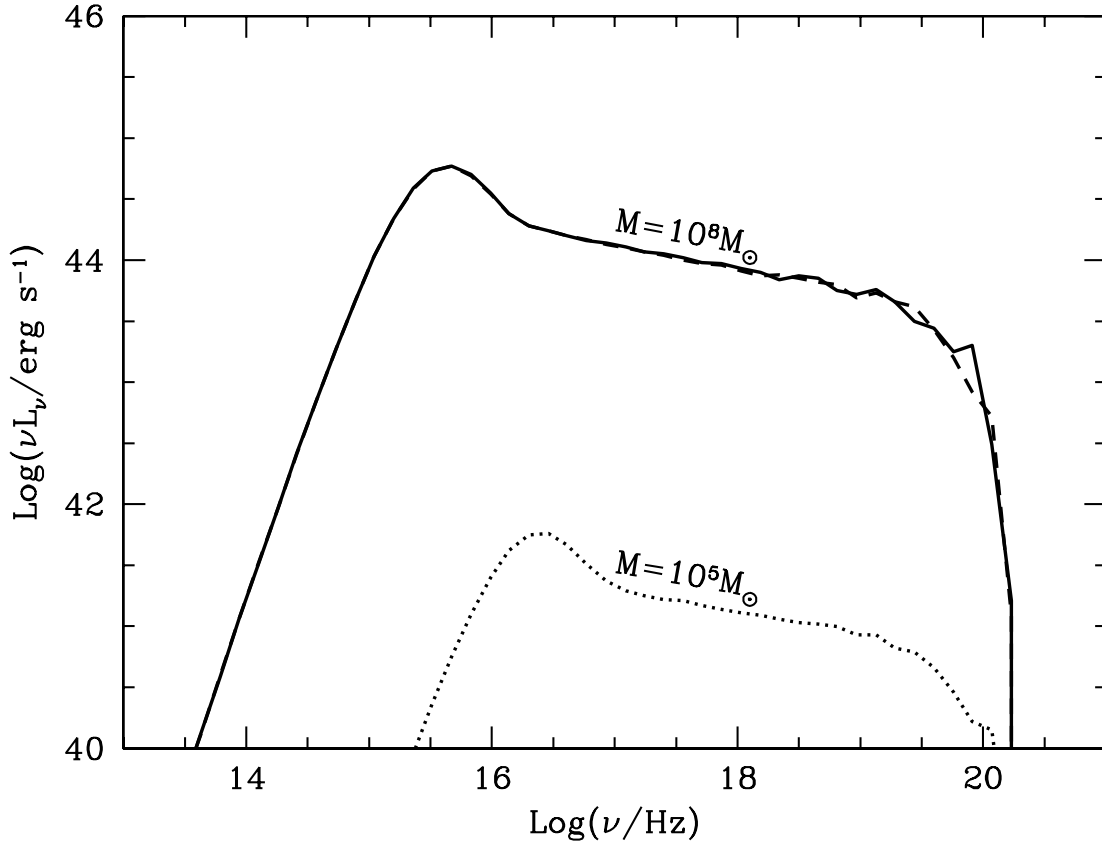


Fig. 8.— The hard-state spectrum for $M = 10^5 M_\odot$ and $\dot{M} = 1\dot{M}_{\text{Edd}}$ (or $L = 0.7L_{\text{Edd}}$) (Dotted curve) compared to that for $M = 10^8 M_\odot$ at same accretion rate $\dot{M} = 1\dot{M}_{\text{Edd}}$ (Solid curve). The spectral shapes are similar except that the disk radiation for $M = 10^5 M_\odot$ is at higher frequency due to higher disk temperature for lower black-hole mass. An example of $\ell = 20R_S$ for $M = 10^8 M_\odot$ and $\dot{M} = 1\dot{M}_{\text{Edd}}$ is also shown in the figure (Dashed curve), which overlaps in the standard case ($\ell = 10R_S$). This indicates that the spectrum hardly changes with the thickness of corona since the hard-state temperature and optical depth given by our model depend on ℓ very weakly.